

## Off-resonant spectral hole burning in CaS:Eu by time-varying Coulomb fields

S. A. Basun,\* M. Raukas,<sup>†</sup> and U. Happek

*Department of Physics and Astronomy, The University of Georgia, Athens, Georgia 30602*

A. A. Kaplyanskii

*A. F. Ioffe Physico-Technical Institute, Academy of Sciences of Russia, 194021, St. Petersburg, Russia*

J. C. Vial

*Laboratoire de Spectrométrie Physique, Université Joseph Fourier and CNRS, Boîte Postale 53X, 38041 Grenoble Cedex, France*

J. Rennie

*Materials and Devices Laboratories, Toshiba Corporation, 1 Komukai, Toshiba-cho, Saiwai-ku, Kawasaki 210, Japan*

W. M. Yen and R. S. Meltzer

*Department of Physics and Astronomy, The University of Georgia, Athens, Georgia 30602*

(Received 9 June 1997)

Persistent spectral hole burning has been observed on the zero-phonon lines of the main site and several perturbed sites of  $\text{Eu}^{2+}$  in CaS:Eu single crystals. Hole burning occurs by two-step photoionization, can be strongly gated with IR irradiation, and takes place by excited-state absorption from the metastable  $4f^65d$  excited state to the conduction band followed by electron transport to  $\text{Eu}^{3+}$  centers which are the dominant traps. A complex hole structure consisting of a narrow feature (200 MHz), and broader features ( $\approx 5$  and  $\approx 100$  GHz) is observed. A mechanism is described for the occurrence of these unusually broad features. Time-varying internal electric fields which occur during the hole burning due to photoionization and trapping can lead to burning of holes at frequencies non-resonant with that of the laser. In addition, a mechanism for hole erasure, tunneling between Eu ions, is demonstrated. This mechanism is identified from the frequency dependence of the hole erasure which follows the  $\text{Eu}^{2+}$  absorption, and the linear dependence of the photoconductivity and hole erasure efficiency on irradiation power, both of which indicate erasure in a single-photon process. [S0163-1829(97)08544-5]

### I. INTRODUCTION

One of the important mechanisms for persistent spectral hole burning (PSHB) in an inhomogeneously broadened zero-phonon line (ZPL) of impurity and defect centers in crystals is photoionization of the centers.<sup>1</sup> Photoionization can result both from one-photon and sequential two-step photoexcitation of the centers (gated hole burning). Photoionization hole burning (HB) is inevitably affected by spatial separation of the electric charges in the crystal lattice occurring in the course of the HB, which causes time varying internal electric fields modifying the energy positions of the electronic levels and the optical transition frequencies of the centers. At the same time, as noted in Ref. 1, we are still far from a detailed understanding of the role of these processes in the formation of the holes and their fundamental properties (spectral width, thermal and optical stability, erasure, etc.). Such an understanding is important for choosing systems for photoionization PSHB which might have application in the domain of optical storage of information.

The goal of the present work is the elucidation of the roles of electron transport processes in the formation and erasure of ionization spectral holes in the example of CaS:Eu. In Sec. II, the spectral and photoconductivity results are described. In Sec. III the HB and hole erasure properties are

presented. Section IV presents a discussion of these results in terms of the electron transport properties.

### II. CaS:Eu—SPECTRAL AND PHOTOELECTRIC PROPERTIES

The single crystals were grown using an arc imaging furnace with a xenon discharge lamp acting as the heat source.<sup>2</sup> The absorption spectrum ( $T < 100$  K) of CaS:0.1% Eu single crystals shows an intense broad band with a long-wavelength ZPL at 625.5 nm (1.99 eV) associated with the transition from the  $4f^7$  ground electron shell to the lowest excited level of the  $4f^65d$  configuration of  $\text{Eu}^{2+}$ . Figure 1 presents a photoluminescence excitation spectrum of the sample at  $T = 2$  K detecting emission from the  $4f^65d$  level, together with the photoluminescence spectrum of this transition consisting of the electron-phonon side band and a strongly reabsorbed ZPL at 625.5 nm. It can be seen from the photoluminescence excitation spectrum (Fig. 1) that it also contains a weak long-wavelength satellite-type continuum with several clearly resolved zero-phonon lines (e.g., at 631.6 and 641.3 nm) corresponding to  $\text{Eu}^{3+}$  ions perturbed by deformation or nearby defects.

Although Eu ions substituting for  $\text{Ca}^{2+}$  ions in the CaS host lattice are expected to be divalent, it is known that

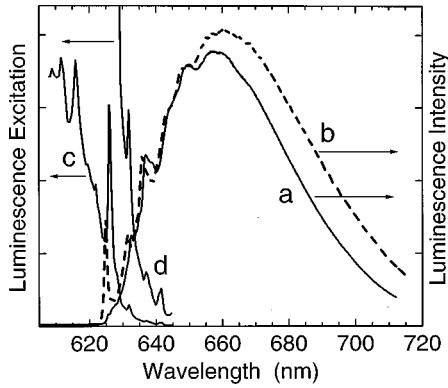


FIG. 1. Curves *a* and *b*: photoluminescence at  $T=2$  K excited with the 514.5-nm Ar-ion laser line. Curves *c* and *d*: photoluminescence excitation spectra excited with tunable dye laser excitation for CaS:0.1% Eu. Curves *a*, *c*, and *d*—single crystal sample; curve *b*—powder, 1% Eu. Curve *d* is curve *c* expanded by factor of 10.

CaS:Eu contains Eu ions in two charge states,  $\text{Eu}^{2+}$  and  $\text{Eu}^{3+}$ .<sup>3</sup> The infrared-absorption spectrum of our samples taken with a Bruker IFS66*v* infrared Fourier spectrometer in the region  $1170\text{--}1250\text{ cm}^{-1}$  shows a single narrow ( $\approx 1\text{ cm}^{-1}$ ) line at  $1204\text{ cm}^{-1}$  (8306 nm)—close to the location of one of the predicted *f-f* transitions between sublevels of the  $\text{Eu}^{3+}$  ground-state multiplet,  ${}^7F_0\text{--}{}^7F_2$ , whose frequency (for powder samples at room temperature) can be roughly estimated as  $1195 \pm 6\text{ cm}^{-1}$ , based on the  $\text{Eu}^{3+}$  luminescence spectrum.<sup>4</sup> This indicates the presence of both charge states of Eu in our samples.

The  $4f^65d$  emitting level of  $\text{Eu}^{2+}$  in CaS is located in the band gap rather close to the conduction-band (CB) bottom. From studies of the temperature-dependent quenching of the  $\text{Eu}^{2+}$  *d-f* photoluminescence, which were interpreted on the assumption that the quenching results from thermal ionization from the  $\text{Eu}^{2+}$   $4f^65d$  excited state to the conduction band, it was estimated that  $\Delta E_{\text{CB}}=0.039\text{--}0.05\text{ eV}$  for thin films, depending on the Eu concentration<sup>5</sup> and  $\Delta E_{\text{CB}}=0.13\text{ eV}$  for bulk samples.<sup>6</sup> In the present work, the separation between the emitting  $\text{Eu}^{2+}$  level and the CB was measured directly from photoconductivity excitation spectra on the single-crystal CaS:0.1% Eu sample under optical irradiation into the  $\text{Eu}^{2+}$  *f-d* absorption band. Figure 2 shows the wavelength dependence of the photocurrents, normalized to the incident photon flux. The photocurrents are linear in incident power. At low temperatures, when thermal ionization from the excited state is suppressed, the photocurrent excitation spectrum rises abruptly (Fig. 2, curve *b*) for wavelengths shorter than 550 nm. We interpret this steep rise as resulting from direct excitation of  $\text{Eu}^{2+}$  to the CB, allowing us to place limits on  $\Delta E_{\text{CB}}$ , i.e.,  $\Delta E_{\text{CB}} < h\nu - h\nu_{\text{ZPL}} = 0.3\text{ eV}$ , where  $\nu$  and  $\nu_{\text{ZPL}}$  correspond to 550 and 625 nm, respectively.

We can obtain  $\Delta E_{\text{CB}}$  more exactly from measurements of the temperature dependence of the photocurrent excited in the region of the *f-d* long-wavelength absorption edge,  $\sim 620\text{ nm}$ . We find that it rises exponentially with temperature, based on measurements between 80 and 300 K, a result which is consistent with the expected temperature dependence,  $j \sim \exp(-\Delta E_{\text{CB}}/kT)$  for combined (photon plus phonon) excitation of  $\text{Eu}^{2+}$  to the CB via the metastable  $4f^65d$

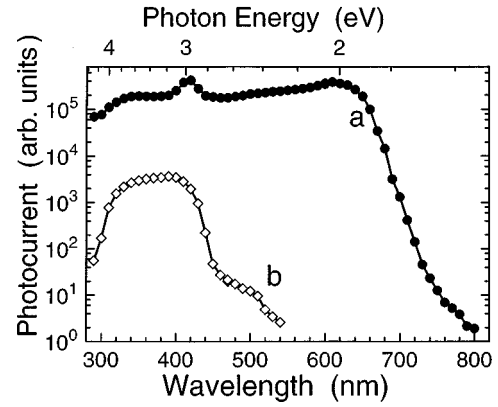


FIG. 2. Stationary photocurrent excitation spectra of a 1-mm single crystal of CaS:0.1% Eu. Curve *a*:  $T=300\text{ K}$  and curve *b*:  $150\text{ K}$ . The photocurrent is normalized to the incident photon flux. The experimental setup was described in Ref. 11.

level. We find  $\Delta E_{\text{CB}}=0.3\text{ eV}$ , in agreement with the value found from the threshold in the photocurrent excitation spectrum.

### III. HB—EXPERIMENT

HB experiments were carried out at  $T=2\text{ K}$ , with a ring dye laser (Coherent Radiation, model 899) resonant with the ZPL. Gating or erasure was accomplished with a tunable broadband dye laser (Coherent Radiation, model 590) or IR light of a 50-W tungsten lamp filtered by cutoff color filters or bandpass interference filters. During the scans, the  $\text{Eu}^{2+}$  phonon sideband emission intensity, selected with a Schott RG665 filter and normalized to the laser beam intensity, was detected by a photomultiplier tube, and recorded with a digital oscilloscope. Thus we were able to measure quantitatively any changes of the initial absorption profile, even when the holes were much broader than the scan range (20 GHz).

PSHB was found to occur on the main ZPL at 625.5 nm, as well as in the whole region between 625.5 and 655 nm containing the continuous absorption tail and on the ZPL's belonging to perturbed  $\text{Eu}^{2+}$  (see Fig. 1). The characteristic features of the PSHB on CaS:Eu observed on the ZPL's at 625.5, 631.6, and 641.3 nm are summarized below.

(i) PSHB on all these lines has a two-photon stepwise character. This follows from the observed quadratic dependence of the burning rate on the ring laser power density (self-gating) at the beginning of burning when the hole depth is much smaller than its saturated value, and also from the observation of two-color gated burning with the additional use of IR light. Figure 3, curve *c* shows a self-gated hole at 625.5 nm, in comparison to the photon-gated hole burned with the simultaneous irradiation with a 50-W tungsten lamp through the Schott RG715 color filter (Fig. 3, curve *d*) during the same period. A strong gating effect is clearly seen. Strong gating is observed even in the presence of tungsten lamp excitation through a Si cutoff filter ( $\lambda > 1.2\mu$ ) implying that  $\Delta E_{\text{CB}} < 1\text{ eV}$ , consistent with the value  $\Delta E_{\text{CB}} \approx 0.3\text{ eV}$  obtained from the photoconductivity measurements of Sec. II.

(ii) The spectral shape of the holes is rather complex and differs between the main (625.5 nm) and satellite lines. On

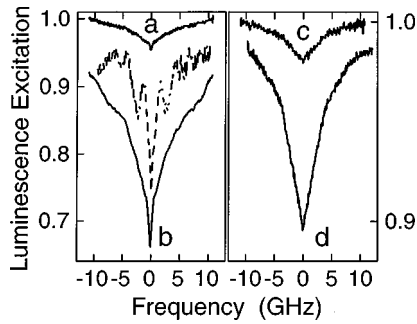


FIG. 3. Persistent spectral holes burned at  $T=2$  K with a power density of  $60 \text{ mW/cm}^2$  incident on a single crystal of  $\text{CaS:0.1\% Eu}$ . Curves *a* and *b*: irradiation at  $631.5 \text{ nm}$  for 3 min. Curves *c* and *d*: irradiation at  $625.5 \text{ nm}$  for 0.5 min. Curves *a* and *c* are self-gated holes, curves *c* and *d* are gated with a tungsten lamp through the Schott RG715 color filter (power density  $\sim 1 \text{ W/cm}^2$ ). Dashed line—spectral hole burned in  $\text{CaF}_2:\text{Eu}^{2+}$  for comparison of hole shape (Ref. 7).

the main ZPL, as well as on the satellite lines, a contour with a full width at half maximum (FWHM) of  $\approx 5 \text{ GHz}$  (see Figs. 3 and 4) is observed, whose spectral shape does not change markedly with hole depth. On the  $631.5\text{-nm}$  ZPL, in addition to the  $5\text{-GHz}$  contour, there also occurs a much narrower hole ( $\approx 200\text{-MHz}$  FWHM) which disappears with increased burning and increased overall hole depth. As the overall hole depth increases, the “main” hole width contour ( $5 \text{ GHz}$ ) remains practically the same, but extended wings appear (ZPL’s of the perturbed sites at  $631.6$  and  $641.3 \text{ nm}$ ) and become deeper (see Fig. 4), extending over a rather broad spectral range to both sides from the resonant frequency ( $\approx \pm 50 \text{ GHz}$ ). These extended wings as well as the narrow  $200\text{-MHz}$  hole are much less pronounced on the main ZPL at  $625.5 \text{ nm}$ .

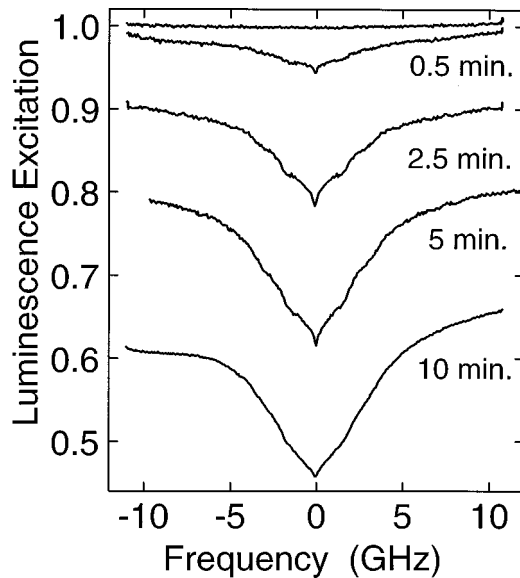


FIG. 4. Sequential burning of a hole at  $T=2$  K and at  $641.3 \text{ nm}$  (incident laser power density of  $60 \text{ mW/cm}^2$ , gating with a tungsten lamp through the Schott color filter RG715) after a total time of 0.5, 2.5, 5, and 10 min. The top trace is the luminescence excitation spectra before burning.

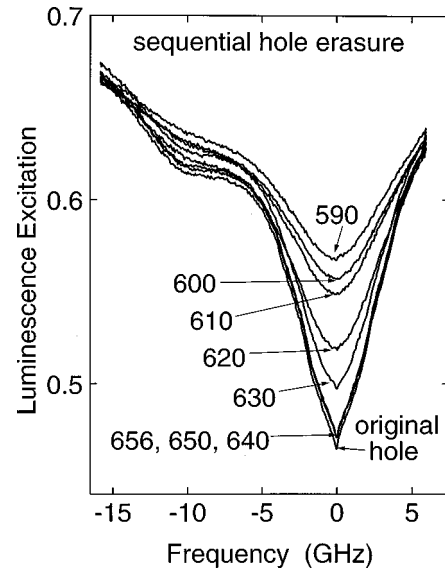


FIG. 5. Sequential erasing (for 5 min each) of the hole burned after 10 min (bottom trace of Fig. 4) with illumination from a tungsten lamp filtered through different interference band pass filters ( $10\text{-nm}$  FWHM):  $656, 650, 640, 630, 620, 610, 600$ , and  $590$ .

(iii) The holes are thermally stable and persist when the sample is heated from  $2 \text{ K}$  to  $T > 100 \text{ K}$ , and kept at the elevated temperature for several tens of minutes. After subsequent cooling down to  $T=2 \text{ K}$ , both the width and depth of the hole remain unchanged.

(iv) The holes can be effectively erased by irradiation of the sample in the spectral region of the  $\text{Eu}^{2+}$  absorption. Figure 5 shows the process of the erasure for the  $641.3\text{-nm}$  site under successive irradiation, each for 5 min, with light of different wavelengths (tungsten lamp plus interference band filters,  $10\text{-nm}$  FWHM). It is seen that effective erasure occurs only for wavelengths shorter than the  $\text{Eu}^{2+}$  ZPL region. Although the erasure is done successively, the main point which is illustrated is the wavelength dependence of the erasure efficiency. In general, during erasure the narrow  $200\text{-MHz}$  feature disappears first, then the  $5\text{-GHz}$  hole fades but almost no change in the extended wings is observed (Fig. 5), i.e., the luminescence remains at a level which is less than  $65\%$  of that before hole burning over the whole  $20\text{-GHz}$  scan range. In Fig. 6, the spectral efficiency of the erasing ( $625.5\text{-nm}$  ZPL), calculated from data similar to that given in Fig. 5, is presented together with the photoluminescence excitation spectrum. There is a clear correlation between the erasure spectrum and the  $\text{Eu}^{2+}$  absorption spectrum. This fact suggests that the  $\text{Eu}^{3+}$  act as traps which become converted to  $\text{Eu}^{2+}$  by capturing the photoionized electrons. It is important to note that the erasure rate was directly proportional to the power of the erasing light, i.e., a one-photon excitation process of  $\text{Eu}^{2+}$  to the  $4f^65d$  state is responsible for the erasure.

(v) Burning of a deep second hole at a different frequency from the first one results in the disappearance of the first hole including the  $\approx 100\text{-GHz}$ -wide pedestal. This supports the ionization character of the holes and the proposed redistribution of  $\text{Eu}$  ions between their charge states,  $\text{Eu}^{2+}$  and  $\text{Eu}^{3+}$ , which occurs during irradiation (see below).

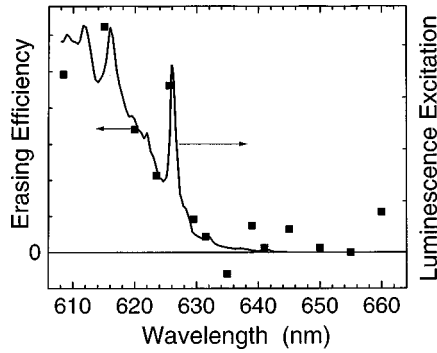


FIG. 6. Comparison of erasure efficiency and  $\text{Eu}^{2+}$  excitation spectrum. Squares—relative erasure efficiency measured on a hole burned on the main site at 625.5 nm and at  $T=2$  K by sequential erasure at different wavelengths (5 min each) with a broadband tunable dye laser (power density 10 mW/cm<sup>2</sup>). Solid line—photoluminescence excitation spectrum from Fig. 1.

#### IV. DISCUSSION

These observations of PSHB on the  $f$ - $d$   $\text{Eu}^{2+}$  ZPL's provide clear evidence of a two-step photoionization mechanism of hole burning in  $\text{CaS}:\text{Eu}$  crystals. The second step, promotion of electrons to the CB, is accomplished either by the same monochromatic light (self-gating) or by IR irradiation (gating). Photoelectrons are captured by traps which we believe are predominantly  $\text{Eu}^{3+}$  ions. Indeed, the presence of electron traps shallower than  $\text{Eu}^{3+}$  ions—if they dominated—would result in a fast erasure of holes under irradiation at the wavelengths longer than  $\text{Eu}^{2+}$  ZPL's, contrary to observations. Thus, selective excitation results predominantly in a spatial redistribution of Eu ions between their charge states,  $\text{Eu}^{2+}$  and  $\text{Eu}^{3+}$  (although some contribution of relatively shallow electron traps should not be ruled out). The large binding energy of the dominant traps ( $\text{Eu}^{3+}$  ions) equal to the ionization energy of  $\text{Eu}^{2+}$ ,  $\approx 2.3$  eV ( $E_{\text{ZPL}} + \Delta E_{\text{CB}}$ ), explains the thermal stability of the holes.

The spectral shape of the holes has a complicated structure which contains both rather narrow features (central 200-MHz hole and a 5-GHz-wide underlying structure) and a very broad ( $\approx 100$  GHz) wings. The  $\approx 5$ -GHz wide structure of both the main hole and holes burned in the perturbed sites, we believe, is associated with sideholes which result from the small crystal-field splitting in the ground state and hyperfine interactions of the  $\text{Eu}^{2+}$  in both the  $4f^7(^8S_{7/2})$  ground state and excited state as observed in  $\text{CaF}_2:\text{Eu}^{2+}$ .<sup>7</sup> For comparison, the hole spectrum observed in  $\text{CaF}_2:\text{Eu}^{2+}$  is reproduced as the dashed line in Fig. 3, where the width of the sidehole structure is seen to be about 5 GHz. The absence of resolved structure compared to that of  $\text{CaF}_2:\text{Eu}^{2+}$  is ascribed to the role of changing internal Coulomb fields which alter (due to the Stark effect) the  $\text{Eu}^{2+}$  optical transition energies due to the photoionization and trapping of the resulting photoelectrons as described below. Zero-field crystal-field splittings of  $\sim 2$ – $5$  GHz for the  $^8S_{7/2}$  ground state of  $\text{Eu}^{2+}$  are common in cubic sites in a number of hosts. As in the case of  $\text{CaF}_2:\text{Eu}^{2+}$ ,<sup>7</sup> the contribution of all ions to the hole at the laser frequency results in the observation of the narrow (200 MHz) central feature in the hole spectrum.

The observation of the broad ( $\sim 100$  GHz) wings on the photoionization hole is a direct manifestation of the photo-

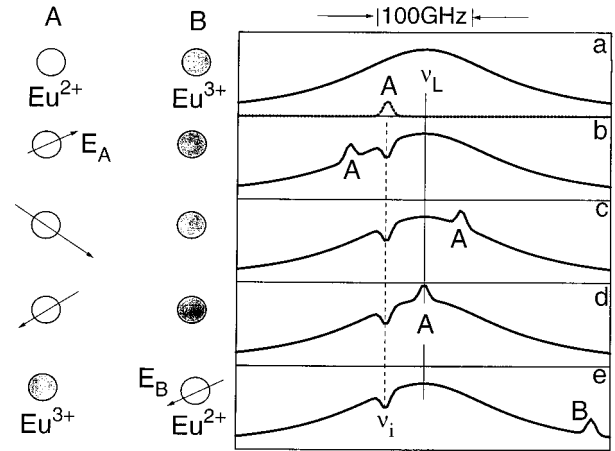


FIG. 7. Schematic illustration of the role of changing internal electric fields in the burning of photoionization spectral holes. Ion A, which initially contributes to the hole at frequency  $\nu_i$ , has its frequency shifted by time-varying Coulomb fields resulting from the ongoing photoionization and trapping of other ions. Eventually, its frequency comes into resonance with that of the laser ( $\nu_L$ ), at which time it is photoionized creating a hole at its original frequency,  $\nu_i$  (see text for detailed description). The ions with their local Coulomb fields are represented by the circles with arrows on the left.

ionization nature of the HB process. We associate the appearance of these wings with the time-varying internal Coulomb fields of Eu ions whose charges are changed due to the photoinduced recharging of ions in the course of HB. To our knowledge, no attention has been paid to the idea that the time varying internal electric fields also results in the *burning of broad holes*, not only in the broadening of the initially narrow holes. Such a dynamic redistribution of optical transition frequencies involves large frequency hops, and thus is distinct from what is usually meant by spectral diffusion.

The process by which the changing internal electric fields result in the broad wings is illustrated in Fig. 7 for two typical ions. Initially (Fig. 7, curve a) ion A is in the 2+ charge state with its ZPL at frequency  $\nu_A = \nu_i$ , and ion B is in the 3+ charge state. Ion B does not initially contribute to the  $\text{Eu}^{2+}$  ZPL, but will eventually trap the photoionized electron from ion A. As the local electric field at ion A changes due to other photoionization processes on other ions with associated movement of charge (Fig. 7, curve b), a hole is created at  $\nu_i$ , and absorption (antihole) appears at the current instantaneous frequency of ion A at  $\nu_A$ . With time  $\nu_A$  can move  $\sim \pm 50$  GHz about  $\nu_L$  within the ZPL contour as the local electric field at A changes [Fig. 7(c)]. Eventually when  $\nu_A = \nu_L$ , the photoionizing laser frequency, ionization results [Fig. 7(d)]. The antihole is now removed and a new absorption (antihole) appears at the resonant frequency of ion B which is now in the 2+ charge state after trapping the electron [Fig. 7(e)]. In general, this ion's resonant frequency is outside the 100-GHz frequency range produced by the time-varying Coulomb fields because of other sources of inhomogeneous broadening (strain, vacancies, dislocations, etc.) which are responsible for the  $30\text{-cm}^{-1}$ -wide ZPL. The net result (Fig. 7, curve e) is that a hole is left at  $\nu_i$ , somewhere within  $\sim \pm 50$  GHz of  $\nu_L$ , and an antihole appears in the

ZPL far removed in frequency from  $\nu_L$ . When one considers the ensemble of Eu ions initially in the 2+ charge state, it is seen that a broad hole is created with a half-width of  $\sim 100$  GHz centered on  $\nu_L$ .

An estimate of the Stark shifts of the  $\text{Eu}^{2+}$  transition frequencies can be obtained using published data on effects of an external electric field  $E_0$  on the  $f$ - $d$  spectral lines of rare earth ions. The quadratic Stark shift of the  $f$ - $d$  ZPL of  $\text{Eu}^{2+}$  ions in cubic centrosymmetric ( $O_h$ ) sites in  $\text{CaF}_2$  is  $5 \times 10^{-13} \text{ cm}^{-1}/(\text{V/cm})^2 E_0^2$ .<sup>8</sup> For the perturbed noncentrosymmetric sites, an estimate can be obtained from results on  $\text{Ce}^{3+}$  centers in  $\text{CaF}_2$  where the cubic symmetry is disturbed by a neighboring charge compensator which destroys the inversion symmetry. The observed Stark effect is  $5 \times 10^{-5} \text{ cm}^{-1}/(\text{V/cm}) E_0$ .<sup>9</sup> The resulting Stark shifts in an electric field of  $E = 10^5 \text{ V/cm}$ , typical of what is expected for the Coulomb field due to a single electron charge in the CaS lattice at mean distances between Eu ions for 0.1% Eu concentrations, is  $\approx 0.1 \text{ cm}^{-1}$  (3 GHz) and  $5 \text{ cm}^{-1}$  (150 GHz) for quadratic (main site) and linear (perturbed sites) Stark effects, respectively. Thus the 100-GHz broad wings in our samples can be explained by the linear Stark effect. This conclusion is supported by the fact that the hole wings are much more pronounced on the ZPL of  $\text{Eu}^{2+}$  ions perturbed by defects and lacking inversion symmetry than for the ZPL of the main sites which have cubic symmetry, and therefore exhibit only quadratic Stark effects.

To support this assumption further, we applied electric fields of up to 22 kV/cm to a hole burned on the 631.5-nm ZPL at zero field. We observed a splitting and broadening of the hole, and the magnitude of the observed Stark effect is adequate to explain the widths of the broad holes on the perturbed sites. Consistent with the absence of a broad hole on the main site, no measurable Stark effect is observed at these fields for holes burned on the main site, as expected for a cubic site. We note that these results are consistent with the previously reported results of Stark effects in  $\text{CaF}_2$  for  $\text{Eu}^{2+}$  and  $\text{Ce}^{3+}$ .<sup>8,9</sup>

We have demonstrated that the selective photoionization of  $\text{Eu}^{2+}$  ions at  $\nu_L$  causes a dynamic spatial redistribution of electric charges in the system of  $\text{Eu}^{2+}$  and  $\text{Eu}^{3+}$  ions. This redistribution results in photoionization of the  $\text{Eu}^{2+}$  ions whose frequencies before irradiation differed from  $\nu_L$  by large values, corresponding to the Stark shifts resulting from changing internal Coulomb fields. This is the origin of the extended wings ( $\approx 100$  GHz). These wings correspond to the transitions of  $\text{Eu}^{2+}$  ions experiencing strong Stark shifts due to their proximity to Eu ions whose charge state changed ( $\pm e$ ) during irradiation. The appearance of the narrow (200 MHz) hole and 5-GHz contour is due to the most recent selective resonant ionization of  $\text{Eu}^{2+}$  ions whose local field and resulting  $f$ - $d$  transition frequencies have not yet changed since its photoionization.

The general origin of the ionization hole erasure under optical excitation is photoinduced recharging of  $\text{Eu}^{2+}$  and  $\text{Eu}^{3+}$ , resulting in spatial redistribution of the 2+ and 3+ charge states in the ensemble of Eu ions. This charge exchange can erase the holes in two ways. In the first, erasure occurs as a frequency redistribution ( $\sim 100$  GHz) of the hole due to variations of the internal Coulomb field, producing Stark shifts of the  $\text{Eu}^{2+}$  transition frequencies which results

in a reduction of the original ‘‘monochromatic’’ components of the hole. It is clear that dissipation of any component of the initial hole must occur fastest for the narrowest components, as was observed (the narrow 200-MHz feature disappears first, then the 5-GHz contour). Due to the large range of frequency hops (comparable with the width of the 100-GHz-wide wings), the erasure of these narrower components of the hole occurs with almost no broadening but rather a redistribution within the 100-GHz feature. Thus the broad  $\sim 100$ -GHz feature is not erased.

In the second but less likely process, some of the  $\text{Eu}^{2+}$  ions previously converted to  $\text{Eu}^{3+}$  and whose absence is responsible for the hole, can be converted back to  $\text{Eu}^{2+}$  (with their  $4f^7 \rightarrow 4f^6 5d$  ZPL frequencies within  $\sim \pm 50$  GHz of those before burning) resulting in partial removal of the broad ( $\sim 100$  GHz) hole. A hole is created by those ions that were photoionized by the broadband erasing light which created the photoelectrons, but the hole frequency can now be anywhere in the ZPL, so that their removal is not perceived as a new hole. This second process occurs for only a small fraction of Eu ions, since it is found that the broad hole is not efficiently erased (see Fig. 5).

What is the mechanism of photoinduced  $\text{Eu}^{2+} \Rightarrow \text{Eu}^{3+}$  recharging resulting from one-photon excitation of  $\text{Eu}^{2+}$ ? The erasure spectrum (Fig. 6) follows the  $\text{Eu}^{2+}$  absorption spectrum, and exhibits a linear power erasure efficiency. The linear erasure efficiency indicates that the dominant mechanism for erasure must be quite different than that for photoionization. We associate this with tunneling of an electron from the excited  $4f^6 5d$   $\text{Eu}^{2+}$  level to a neighboring  $\text{Eu}^{3+}$ . The existence of such tunneling is independently supported by the observation of a photocurrent that is linear in laser irradiation power at  $T = 2 \text{ K}$ , whose excitation spectrum follows the  $\text{Eu}^{2+}$  absorption spectrum in the region of the main ZPL and shorter wavelengths. Such processes of electron tunneling from impurity excited states were observed also in other systems (photorecharging of Cr ions in ruby,<sup>10</sup> HB on color centers<sup>1</sup>), and they efficiently occur over rather large distances. Even in  $\text{Al}_2\text{O}_3:\text{Cr}^{3+}$  (ruby)—where the excited  ${}^2E$  level of  $\text{Cr}^{3+}$  is located very deep in the band gap and thus its wave function is very compact—the tunneling efficiently occurs over several nanometers.<sup>10</sup> For  $\text{Eu}^{2+}$  ions in CaS, the proximity of the  $\text{Eu}^{2+}$   $4f^6 5d$  level to the CB should be taken into account, which strongly affects the extension of the  $\text{Eu}^{2+}$   $4f^6 5d$  level wave function in CaS, contrary to the cases of the systems such as  $\text{CaF}_2:\text{Eu}^{2+}$ , with  $\Delta E_{\text{CB}}$  on the order of several eV.

The tunneling which provides the main contribution to hole erasure in CaS:Eu should also contribute to the HB where, as mentioned above, two-photon ionization dominates. However, tunneling is favored for hole erasure, since the erasing light is broadband and is therefore nonselective, exciting the  $f$ - $d$  transition for all  $\text{Eu}^{2+}$  ions with equal probability. The system of  $\text{Eu}^{2+}$  ions can then self-select those ions with nearby  $\text{Eu}^{3+}$  electron acceptor sites where tunneling is highly probable. The resulting photoionization generates time-varying fields. In contrast, under selective excitation during the HB, only a very small fraction of those  $\text{Eu}^{2+}$  ions resonant with the laser will be in favorable locations for tunneling, especially if the Eu exist predominantly in the  $\text{Eu}^{2+}$  state as we believe. However, two-photon ionization to

the conduction band provides mobility to the electron, allowing it to seek a more distant  $\text{Eu}^{3+}$  acceptor, thereby making photoionization available to a large fraction of the resonant  $\text{Eu}^{2+}$  centers.

## V. CONCLUSIONS

Infrared photon-gated burning of persistent spectral holes is reported in  $\text{CaS:Eu}$ . The holes exhibit a complex structure consisting of a narrow feature (200 MHz), and broader features ( $\sim 5$  and 100 GHz). A mechanism for the formation of the anomalously broad spectral holes is demonstrated; time-varying Coulomb fields resulting from the photoionization lead to hole burning at frequencies nonresonant with that of

the excitation. A hole erasure mechanism in this system is unraveled. Hole erasure results from electron tunneling between  $\text{Eu}^{2+}$  and  $\text{Eu}^{3+}$  ions, consistent with our findings that hole erasure occurs in a one-photon process, and that the frequency dependence of the erasure rate follows the  $\text{Eu}^{2+}$  absorption spectrum. Direct evidence of tunneling between Eu ions is given by photoconductivity measurements.

## ACKNOWLEDGMENT

We acknowledge the support of the National Science Foundation through Grant Nos. DMR-9307610, DMR-9321052, and DMR-9424216.

\*On leave from the A. F. Ioffe Physico-Technical Institute, St. Petersburg, Russia.

<sup>†</sup>Present address: Osram Sylvania, Inc., Research and Development, 71 Cherry Hill Rd., Beverly, MA 01915.

<sup>1</sup>R. M. Macfarlane and R. M. Shelby, in *Persistent Spectral Hole Burning: Science and Applications*, edited by W. E. Moerner (Springer-Verlag, Berlin, 1988), p. 127.

<sup>2</sup>Y. Kaneko, K. Morimoto, and T. Koda, *J. Phys. Soc. Jpn.* **51**, 2247 (1982).

<sup>3</sup>M. Pham-Tai, *J. Alloys Compd.* **225**, 547 (1995); M. Pham-Tai, *Jpn. J. Appl. Phys.* **31**, 2811 (1992).

<sup>4</sup>N. Yamashita, S. Fukumoto, S. Ibuki, and H. Ohnishi, *Jpn. J. Appl. Phys.* **32**, 3135 (1993).

<sup>5</sup>K. Swiatek, M. Godlewski, L. Niinistö, and M. Leskelä, *J. Appl.*

*Phys.* **74**, 3442 (1993); K. Swiatek, K. Karpinska, M. Godlewski, L. Niinistö, and M. Leskelä, *J. Lumin.* **60&61**, 923 (1994).

<sup>6</sup>M. Ando and Y. A. Ono, *J. Cryst. Growth* **117**, 969 (1992).

<sup>7</sup>D. M. Boye, R. M. Macfarlane, Y. Sun, and R. S. Meltzer, *Phys. Rev. B* **54**, 6263 (1996).

<sup>8</sup>A. A. Kaplyanskii and V. N. Medvedev, *Opt. Spektrosk.* **23**, 404 (1965) [*Opt. Spectrosc.* **23**, 743 (1967)].

<sup>9</sup>A. A. Kaplyanskii and V. N. Medvedev, *Pis'ma Zh. Eksp. Teor. Fiz.* **2**, 209–212 (1965) [*JETP Lett.* **2**, 133 (1965)].

<sup>10</sup>A. A. Kaplyanskii, S. A. Basun, and S. P. Feofilov, *J. Lumin.* **38**, 120 (1987).

<sup>11</sup>W. M. Yen, M. Raukas, S. A. Basun, W. van Schaik, and U. Happek, *J. Lumin.* **69**, 287 (1996).